Malaysian Journal of Analytical Sciences (MJAS)
Published by Malaysian Analytical Sciences Society

PHYSICAL AND ELECTROCHEMICAL CHARACTERISTICS OF $LiCo_{0.6}Sr_{0.4}O_2$ CATHODE INK FOR INTERMEDIATE-LOW TEMPERATURE SOLID OXIDE FUEL CELL

(Pencirian Fizikal dan Elektrokimia Terhadap Dakwat Katod $LiCo_{0.6}Sr_{0.4}O_2$ bagi Sel Fuel Oksida Pepejal Bersuhu Sederhana Rendah)

Nur Nadhihah Mohd Tahir[1], Nurul Akidah Baharuddin[1]*, Wan Nor Anasuhah Wan Yusoff[1], Azreen Junaida Abd Aziz[1], Mahendra Rao Somalu[1], Andanastuti Muchtar[1,2]

[1]Fuel Cell Institute
[2]Department of Mechanical and Manufacturing Engineering, Faculty of Engineering and Built Environment Universiti Kebangsaan Malaysia, 43600 UKM Bangi, Selangor, Malaysia

**Corresponding author: akidah@ukm.edu.my*

Received: 30 November 2021; Accepted: 27 February 2022; Published: 27 June 2022

Abstract

Solid oxide fuel cell (SOFC) is a technology used to generate electricity with less emission. Selection of a suitable, compatible cathode material that will be used with the ionic and protonic electrolyte is crucial in achieving an excellent performance of intermediate-low temperature SOFC. $LiCo_{0.6}Sr_{0.4}O_2$ (LCSO) is stoichiometrically prepared via glycine nitrate combustion followed by ball milling and triple roll mill (TRM) machine to produce a homogeneous LCSO cathode ink. The prepared sample powder of LCSO is initially characterised by X-ray diffraction (XRD) and scanning electron microscope (SEM) fitted with energy-dispersive X-ray spectroscopy. The XRD demonstrated that the prepared LCSO powder calcined at 800 °C shows a phase structure of rhombic lattice and space group of R-3m. The prepared ink is then layered on both sides of the samarium-doped-ceria (SDC) electrolyte to produce LCSO | SDC | LCSO symmetrical cell. The prepared ink has varied gap sizes on the TRM machine. The electrochemical performance of electrochemical impedance spectroscopy reports that the best gap size is at 40 µm with the lowest polarisation resistance (R_p), of 8.32 Ω. In conclusion, this work confirms the importance of a high-quality lithium-based cathode ink in SOFC applications.

Keywords: solid oxide fuel cell, cathode, ink, lithium, triple roll mill

Abstrak

Sel fuel oksida pepejal (SOFC) boleh dikategorikan sebagai teknologi pembebasan karbon rendah dalam menjana tenaga elektik. Pemilihan bahan katod yang sesuai dan serasi untuk digunakan bersama dengan elektrolit ionik dan protonik adalah penting dalam mencapai prestasi SOFC bersuhu sederhana-rendah (IT-LT SOFC) yang baik. $LiCo_{0.6}Sr_{0.4}O_2$ (LCSO) telah disediakan mengikut stoikiometri menggunakan pembakaran glisin nitrat diikuti dengan pengisaran bebola dan pengisaran tiga penggelek untuk menghasilkan dakwat katod LCSO yang homogen. Serbuk sampel LCSO yang disediakan pada mulanya dicirikan menggunakan pembelauan sinar-X (XRD) dan mikroskop elektron pengimbasan (SEM) yang dipasang dengan spektroskopi sinar-X penyebaran tenaga (EDX). Hasil dapatan XRD menunjukkan kalsin serbuk katod LCSO yang disediakan pada 800 °C menunjukkan struktur

fasa kekisi Rhombo dan kumpulan ruang R-3m Dakwat yang disediakan kemudiannya disapukan pada kedua-dua belah elektrolit samarium terdop seria (SDC) untuk menghasilkan sel simetri LCSO | SDC | LCSO. Dakwat yang disediakan dipelbagaikan saiz celah mesin gulung tiga. Daripada prestasi elektrokimia spektroskopi impedans elektrokimia (EIS) melaporkan bahawa saiz celah terbaik adalah pada 40 µm dengan rintangan polarisasi terendah, R_p 8.32 Ω Kesimpulannya, kajian ini mengesahkan kepentingan dakwat katod berasaskan litium berkualiti tinggi dalam aplikasi SOFC.

Kata kunci: sel fuel oksida pepejal, katod, dakwat, litium, pengisar tiga penggelek

Introduction

Fuel cells are currently receiving great attention worldwide due to their claim of being the safest and cleanest technology [1]. A fuel cell can also be considered an efficient power generator due to lesser emission and a higher rate of energy conversion efficiency compared with conventional internal combustion engines. Lina et al. stated that a fuel cell is a clean power generator with less noise pollution [2]. Fuel cells have several types, and this work explains solid oxide fuel cell (SOFC) in detail. Nowadays, SOFC is well-known in the technological and industrial fields. The only identification that distinguishes SOFC from other types of fuel cells is that they operate at a high temperature, ranging from 400 °C to 1000 °C [3–5]. SOFC is an energy conversion device that can convert chemical energy derived from the fuel into electrical and thermal energy [6,7].

SOFC consists of three main components: anode, cathode and electrolyte. The anode and the cathode are known as an electrode–electrolyte layer that is sandwiched between the anode and cathode electrodes [8]. The schematic of the SOFC is shown in Figure 1.

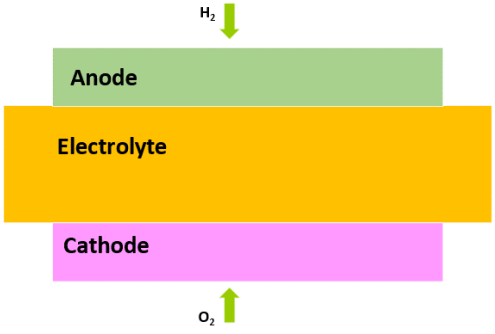

Figure 1. Schematic of SOFC

SOFC has a high energy efficiency when operating at a high temperature of 1000 °C [9, 10]. Studies show that SOFC can achieve an efficiency of 60%–65%. On the one hand, SOFC has been declared as the most promising power generation technology due to its variety of advantages. On the other hand, the high operating temperature which causes material degradation and an increase in manufacturing cost, also results in poor durability of SOFC and limits its application [11]. Accordingly, selection of an intermediate-low temperature is crucial to overcome these arising issues on high operating temperature. The temperature range of intermediate-low temperature is 400 °C–700 °C [12]. The operating cost of this device will be reduced by lowering its temperature, thereby enhancing its commercialisation. SOFC has two types of environments: oxide-conducting SOFC (O^{2-}-SOFC), which is the pioneer or conventional type, and proton-conducting SOFC (H^+-SOFC). Figure 2 (a) and (b) show the O^{2-}SOFC and H^+-SOFC, respectively.

Currently, the focus of SOFC development is on intermediate-low temperature SOFC (IT-LT SOFC). However, the high operating temperature of SOFC causes cell degradation issues. To overcome this problem, the operating temperature of SOFC should be reduced to 400-800 ℃. Existing materials that have been traditionally operated at elevated temperatures have poor electrochemical performance under this intermediate-low temperature environment. Accordingly, selection of a suitable and compatible cathode material is crucial for IT-LT SOFCs. Lithiated-based materials are one of the strong candidates for the cathode component of IT-LT SOFCs. The lithiated-based cathode has been widely used in many applications, such as batteries, electrochemical capacitors and O_2 metal batteries [13–22]. The lithiated-based material in SOFC provides a free moving lithium-

ion (Li^+) cation pathway [23]. The lithium-based cathode can be categorised as a triple ($H^+/O^{2-}/e^-$) conducting cathode material, indicating that it can allow those three conducting elements to pass through the cathode boundary or cathode active site [24]. Liu et al. stated that lithium cobaltite, $LiCoO_2$ is one of the promising lithiated-based materials to be used in SOFC applications with triple conducting mechanism capabilities [25,26]. Wan Yusof [27] reported that $LiCoO_2$ or lithium-based material shows a reasonable perspective in intermediate to low temperature for proton- and oxide-conducting SOFC applications [28]. Moreover, strontium (Sr) is widely used as a cathode dopant for most cathode materials to achieve high electrocatalytic activity, especially at the oxygen reduction reaction (ORR) that occurs only in the cathode [29]. Jamil et al. adopted a broad perspective, in which the existence of an Li compound may uplift oxygen concentration, especially at the grain boundary, resulting in high ionic conductivity [30]. Li^+ promotes proton transfer, which makes Li-based cathode materials viable for proton-conducting IT-LT SOFC. Improving the performance of this material requires an in-depth study of the powder and ink preparation aspects. Meanwhile, numerous studies have been conducted on the powder synthesis-related parameters. As previously discussed, a huge gap was observed on the ink production-related parameters. Hence, this study aims to produce a high-quality lithiated-based cathode ink ($LiCo_{0.6}Sr_{0.4}O_2$) by altering the gap size of roller in triple-roll mills and to characterize the physical properties and electrochemical performance of the cathode inks for IT-LT SOFC application. The high-quality cathode ink will be produced with a triple roll mill machine, which has been proven to be the optimum method for ink production.

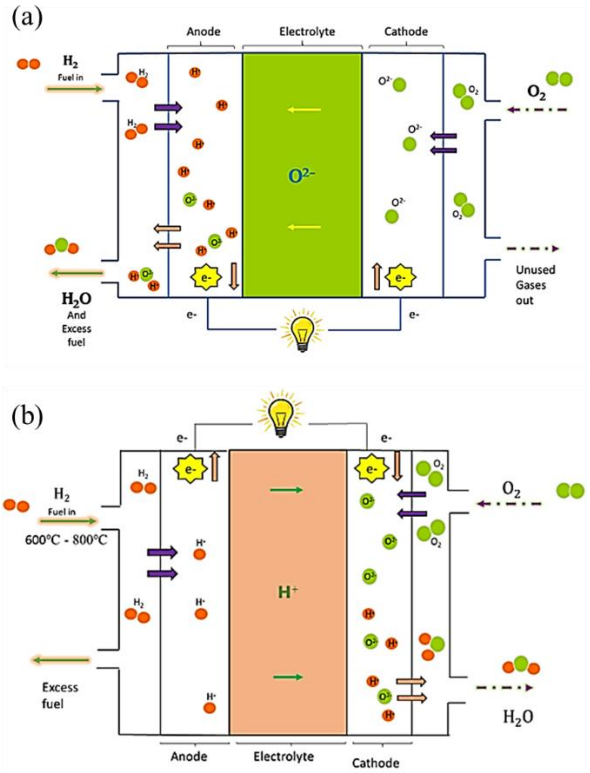

Figure 2. (a) O^{2-}SOFC and (b) H^+-SOFC

Materials and Methods

Preparation of cathode sample powder LiCoSrO

In this work, $LiCo_{0.6}Sr_{0.4}O_2$ precursor powders were produced through the glycine nitrate combustion method. The precursor materials were Lithium Nitrate ReagentPLus, $LiNO_3$ (Sigma Aldrich, Germany), Strontium Nitrate (ACS Reagent, >99%) $Sr(NO_3)_2$ (Sigma Aldrich, Germany) and Cobalt (II) Nitrate Hexahydrate Reagent Grade, 98%, $Co(NO_3)_2.6H_2O$ (Merck Chemicals, Germany). A stoichiometric amount of the precursor materials was dissolved in 100 mL deionised water and stirred for 40 min on a hotplate with a magnetic stirrer at room temperature. Afterwards, a calculated amount of glycine (Sigma–Aldrich, Germany) was added to the precursor material solution as fuel. The mixture was continuously stirred on the hotplate at room temperature for 18 h. Subsequently, the solution was continuously stirred whilst the temperature of the hotplate was slowly increased to between 250 °C to 300 °C to achieve the combustion of the materials and all the nitrates. Thereafter, the obtained black ash precursor powder was further dried at 120 °C for 12 h in

a drying oven. The raw powder was then ground using a mortar agate to obtain a fine, smooth powder. Finally, the dried fine precursor powder was calcined at 800 ℃ in a high-temperature furnace (Berkeley Scientific, USA) for 5 h holding time. The TGA graph of the previous study [27] on the same material shows that LCSO materials were decomposed at temperatures ranging from 700 – 1000 ℃. After the LCSO powder was calcined, it was subjected to X-ray diffraction (XRD) testing and scanning electron microscope (SEM) analysis for LCSO its characterisation.

Material characterisation

Wan Yusoff et al. [27] investigated the thermal decomposition behaviour of the LCSO powder in 2020, via thermogravimetric analysis/differential scanning calorimetry (TGA/DSC, SING Mettler Toledo, United States) to determine the optimal calcination temperature. The analysis was conducted on the LCSO precursor powder synthesised from room temperature to 1000 °C at a heating rate of 10 °C/min^{-1} under air with a flow rate of 50 mL/min^{-1}. Then, the precursor LCSO powder was further analysed via XRD (Bruker AXS D8 Advance, Germany) with a CuKα (λ = 0.15406 nm) radiation source to confirm its phase and structure. An X-ray diffractometer was operated at 40 kV and 40 mA, and fitted with a 1-D fast detector (Lynx-Eye). The XRD spectrum was recorded for 2θ ranging from 20° to 70° with a step size of 0.025°. The morphology of the LCSO particles was examined via SEM (Carl Zeiss EVO MA10, Germany). From the material characterisation, the optimal calcination temperature was selected to produce another batch of LCSO cathode powder, which was used to synthesise the LCSO cathode ink.

Ink preparation

The cathode ink was produced using several methods and techniques that have been utilized by other researchers. The common methods used for synthesizing the ink are triple roll mill (TRM) machine, ball milling and manual mixing (hands-on). The methods used by other researchers are summarised in Table 1.

Table 1. Summary of methods used to produce ink

Method	Element	Performance	Reference
Ball Milling	Iron and nitrogen dope carbide-derived carbon (SiCDC)	The grain size decreases from 1 μ to 200 nm.	Ratso et al. 2021[31]
	Multiwalled carbon nanotubes/epoxy suspensions	A better-quality texture of the material is produced.	Olowojoba et al. [32]
TRM Machine	Soda lime glass	Fast response and process can be broken down into phases. The particle size breakage yields a good result.	Böttcher et al. [33]
	$La_{0.6}Sr_{0.4}CoO_{3-\delta}$ (LSC)	High porosity and good electrochemical performance are achieved with a TRM machine.	Samat et al. [10]
Manual Mixing	$La_{0.6}Sr_{0.4}CoO_{3-\delta}$ (LSC)	The porosity is lower, and the value of ASR is higher compared with other methods.	Samat et al. [34]

Table 1 shows that using the TRM machine as the medium in synthesising the cathode is the best option because if the better quality and outstanding electrochemical performance. Several parameters in the ink production process are maintained variable during the research. Determining and varying the parameters is crucial to producing a high-quality cathode ink. Table 2 shows the parameters considered and previously studied. The parameters studied by the researchers include roller speed, frequency of rotation, roller gap size, ink thickness, feed rate and breakage behaviour.

Table 2. Parameter study related to the TRM machine

Parameter study related to the TRM	Reference
Roller gap size	Wan Yusoff et al. [27]
Roller speed and rotation frequency	Olowojoba et al. [32]
Roller speed, roller gap size, feed rate and breakage behaviour	Böttcher et al. [33]
Ink thickness	Samat et al. [34]
Roller speed and roller gap size	Somalu et al. [35]

TRM is essential in the production of homogenous screen-printing inks because it breaks down most particle agglomerates during milling. The difference in roller speeds produces shear stress between the rollers, which pull agglomerates apart when the material passes between the gaps. The working principle of the TRM machine is shown in Figure 3. The resulting shear rates between the gaps are provided in the following equation:

$$\text{Shear rate} = \frac{\Delta v}{x}, \quad (1)$$

Δv: speed difference, and x: gap between rollers.

The LCSO ink was prepared with EXAKT 50 I, Germany TRM machine in the SOFC Laboratory at Institute Fuel Cell UKM. The produced LCSO powder was ball-milled for 24 h with a 10-rpm rotating rate. The ink was prepared by using the right composition to produce a good-quality cathode ink. The ink composition is tabulated in Table 3. The postball milled LCSO powder was mixed with a vehicle buffer solution, dispersant and solvent. The premixed ink was manually ground before producing a smooth, fine ink with the TRM machine. Then, all the premixed ink was mixed well. The LCSO with various ink parameters were formed, and the parameters produced throughout this work are listed in Table 4.

Table 3. LCSO ink composition

Solid Content	Weigh (wt.%)
LCSO powder (ball milled)	67.33
Solvent (Terpineol)	29.98
Binder (Ethylcelulose N7 grade (0.25%–0.5 wt.%)	1.35
Dispersant (Hypermer KD15)	1.35

Table 4. LCSO ink parameter

Variable Parameter	Gap Size (μm)
1	g_1- 10
2	g_2- 20
3	g_3- 30
4	g_4- 40
5	g_5- 50

Fabrication of symmetrical cell LCSO|SDC|LCSO

The fabrication of symmetrical cell started with the production of an electrolyte pellet of $Sm_{0.2}Ce_{0.8}O_{1.9}$ (SDC). Then, the prepared LCSO cathode ink was layered on both sides of the electrolyte pellet. Prior to the half and symmetrical cell production for electrical conductivity and electrochemical impedance spectroscopy (EIS) analysis, the SDC powders (Sigma–Aldrich) were pressed into a coin-shaped structure to form an electrolyte substrate at 52 MPa. The SDC electrolyte was sintered at 1400 °C for 6 h. Then, the as-prepared cathode inks were screen printed two layers on one side (half-cell) and both sides (symmetrical cell) of the electrolyte surface with an active area, A, of 1 cm^2 prior to sintering at 800 °C for 2 h. The prepared symmetrical cell LCSO|SDC|LCSO is shown in Figure 3.

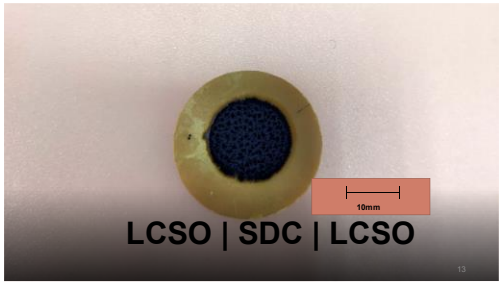

Figure 3. Prepared symmetrical cell LCSO|SDC|LCSO

Electrochemical analysis of the LCSO|SDC|LCSO symmetrical cell

The electrochemical performance was measured using EIS with a potentiostat (PGSTAT302 N, Metrohm Autolab, Netherlands) operating at 106–0.1 Hz with a sinusoidal voltage amplitude of 10 mV. Symmetrical cells were evaluated in the air at 500 °C–800 °C under typical IT-SOFC operating conditions, with a constant air flow rate of 0.2 $Lmin^{-1}$. EIS was performed on all symmetrical cells with a constant active area of 1 cm^2, and the data were processed with NOVA software (version 1.10) to determine the ASR values of the LCSO cathode.

Results and Discussion

Properties of prepared powder

The XRD spectrum of the as-synthesised powder cathode calcined at 800 °C and 900 °C for 5 h is shown in Figure 4. The data base cannot provide the full spectrum of LiCoSrO because this material is new. Accordingly, the XRD was compared with $LiCoO_2$ and $SrCO_3$. The calcined LCSO powders exhibited merely a single phase, as confirmed by the XRD measurement. The plotted results showed a peak almost similar to the reference $LiCoO_2$ with $SrCO_3$. All the prominent peaks in the XRD spectrum of the calcined powder were matched with the reference code PDF 00-050-0653 lithium cobalt oxide ($LiCoO_2$) of rhombic lattice structure and space group of R-3m and PDF 01-084-1778 strontium carbonate ($SrCO_3$) of orthorhombic lattice structure with space group of R-3m. Thus, the highest peaks were indexed to their Miller indices (hkl) of (111) and (104) for $LiCoO_2$ and $SrCO_3$, respectively.

The morphological analysis was conducted on the LCSO powders calcined at temperatures of 800 °C and 900 °C by SEM and EDX. The results for both microstructures are illustrated in Figures 5 and 6. The results show that the microgram has a random fragment structure, whereas EDX confirms that all the components of LCSO are in the cathode powders. The EDX graph in Figure 6 clearly shows that all the components of Li, cobalt (Co), strontium (Sr) and oxide (O_2) are present in the LCSO powder for both temperatures of calcined LCSO. However, the LCSO precursor powder calcined at a temperature of 800 °C shows less impurities than that calcined at 900 °C.

After analysing the calcined powder and producing a high-quality ink, the best composition was considered. Based on the LCSO ink composition in Table 3, the smooth, fine-texture ink was successfully produced using the in-house TRM machine. The produced LCSO cathode ink is shown in Figure 7.

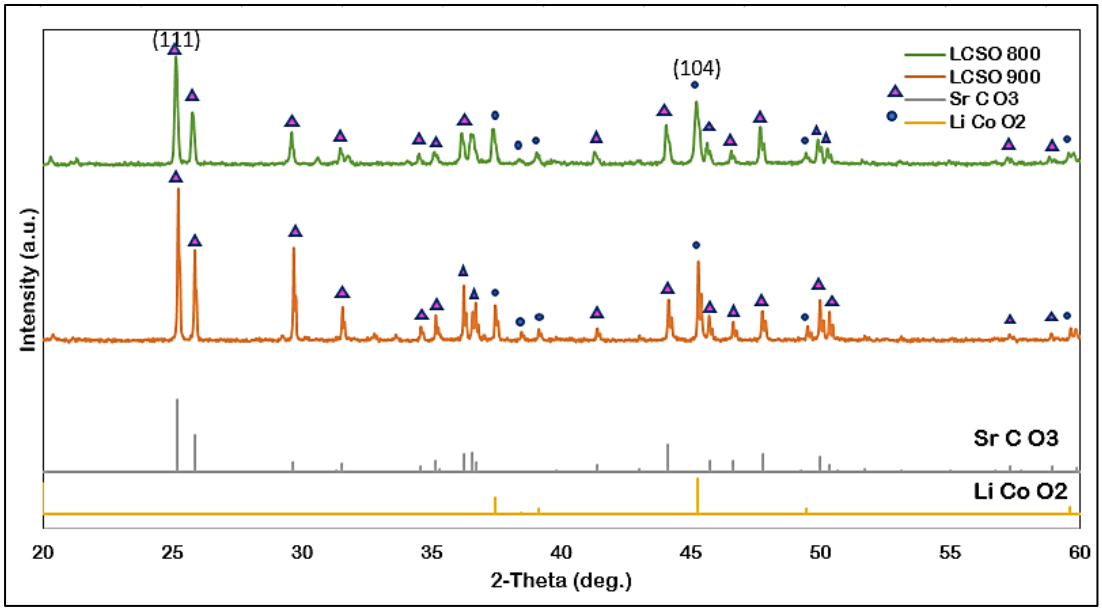

Figure 4. XRD spectrum obtained by this research

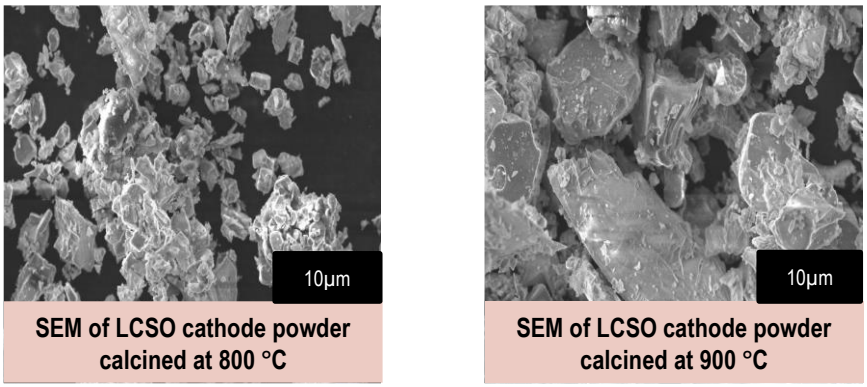

Figure 5. SEM of the LCSO powder calcined at temperatures of 800 °C and 900 °C

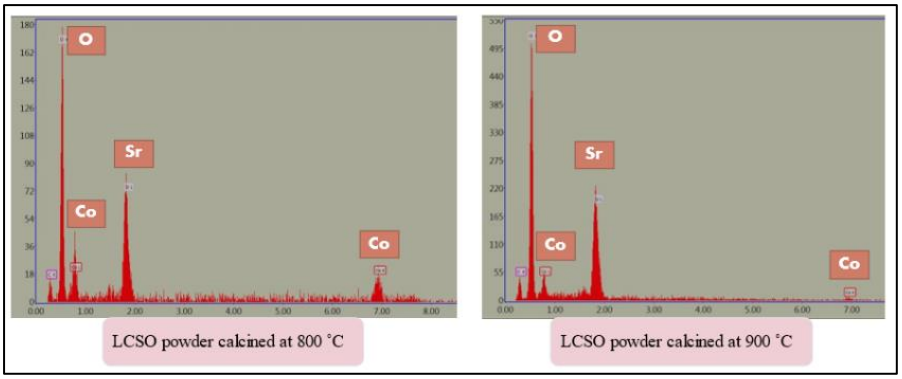

Figure 6. EDX analysis of the calcined LCSO powder

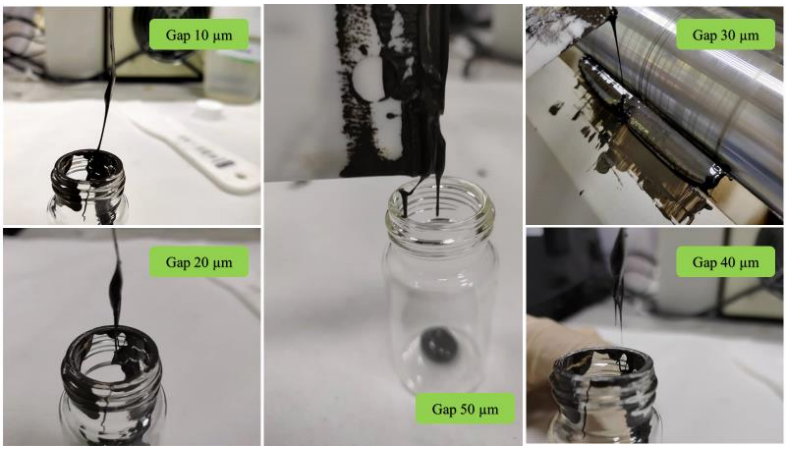

Figure 7. Produced LCSO cathode ink

Electrochemical performance analysis

Figure 8 shows the electrochemical impedance spectrum of the LCSO|SDC|LCSO symmetrical cells with different cathode ink parameters of the gap size of the TRM. The spectra are fitted via electrical circuit fitting composed of resistance (R) and constant phase element (CPE). Resistances and constant phase elements are illustrated by R_S, R_1, R_2, CPE_1 and CPE_2 for high- and low-frequency arcs. The impedance arc was analysed using an electric equivalent circuit, as shown in Figure 8(b). All the measured and calculated values of polarisation resistance and area specific resistance (ASR) at 800 °C of each symmetrical cell with different gap size are listed in Table 5. The impedance spectra in Figure 8(a) show that gap size of 40 µm is the lowest amongst the other gap sizes, and this is proven by the measured and calculated polarisation resistance, R_p, value in Table 5 that shows the gap sizes of 10, 20, 30, 40 and 50 µm of 32.35, 39.63, 17.07, 8.32 and 43.36 Ω, respectively. The LCSO cathode ink produced with the TRM shows that the best gap size is 40 µm with proven electrochemical performance of 8.32 Ω.

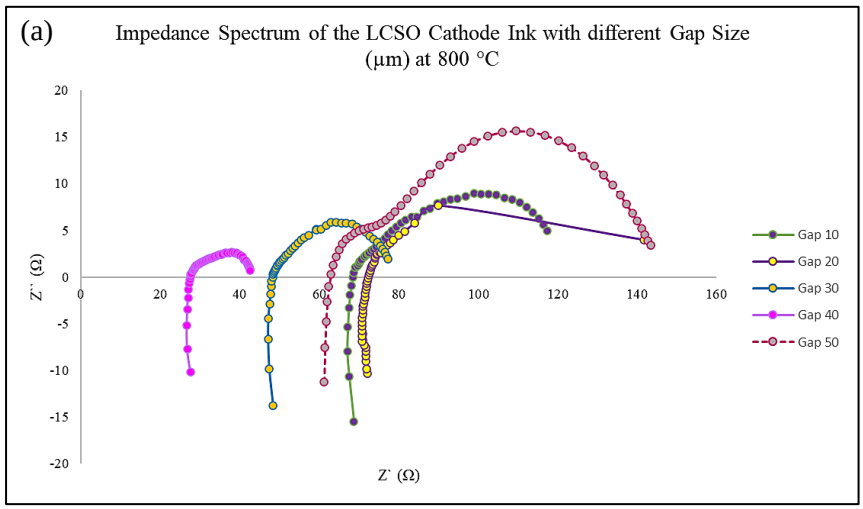

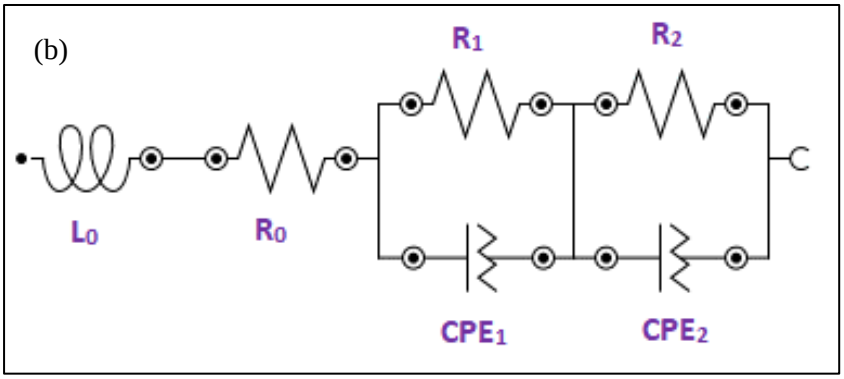

Figure 8. (a) Impedance spectra of the different gap sizes; (b) adopted an electrical equivalent circuit to analyse the impedance data

Table 5. Values of the polarisation resistance and ASR of LCSO|SDC|LCSO symmetrical cells of different gap sizes of the ink produced

Gap Size (μm)	Polarisation Resistance, Rp (Ω)	ASR at 800 °C (Ω cm^2)
10	32.35	16.175
20	39.63	19.815
30	17.07	8.535
40	8.32	4.160
50	43.36	21.680

Conclusion

The LCSO cathode ink is synthesised via glycine nitrate combustion. Subsequently, the cathode ink was produced using the TRM machine method, and the gap size of the TRM varied at 10, 20, 30, 40 and 50 μm. Amongst the different gap sizes, the best gap size is 40 μm with proven electrochemical performance of EIS with polarisation resistance, R_p value of 8.32 Ω and ASR of 4.160 Ωcm^2. This work benchmarks the attempt of a compatibility of an Li-based cathode ink in the application of IT-LT SOFCs. Moreover, this work is involved in and will compete in the production of a durable SOFC system to enhance its viability in actual applications. In the future, the production of the LCSO cathode ink under various IT-LT SOFC environments, such as proton conducting SOFC (H^+-SOFC) and oxide conducting SOFC (O^{2-}SOFC) will be conducted to find the optimal environment for LCSO cathode ink to work for.

Acknowledgement

The authors gratefully acknowledge the financial support provided by the Ministry of Higher Education, Malaysia and the funding support via the research sponsorship under Fundamental Research Grant Scheme grant number FRGS/1/2019/TK07/UKM/02/1 and Universiti Kebangsaan Malaysia through Research Grant DIP-2010-011.

References

1. Ali, S. M., Anwar, M., Abdalla, A. M., Somalu, M. R. and Muchtar, A. (2017). Ce0.80Sm0.10Ba0.05Er0. 05O2-δ multi-doped ceria electrolyte for intermediate temperature solid oxide fuel cells. *Ceramics International,* 43(1): 1265-1271.

2. Rashid, N. L. R. M., Samat, A. A., Jais, A. A., Somalu, M. R., Muchtar, A., Baharuddin, N. A. and Isahak, W. N. R. W. (2019). Review on zirconate-cerate-based electrolytes for proton-conducting solid oxide fuel cell. *Ceramics International,* 45(6): 6605-6615.
3. Baharuddin, N. A., Abdul Rahman, N. F., Abd. Rahman, H., Somalu, M. R., Azmi, M. A. and Raharjo, J. (2020). Fabrication of high-quality electrode films for solid oxide fuel cell by screen printing: a review on important processing parameters. *International Journal of Energy Research,* 44(11): 8296-8313.
4. Abd Aziz, A. J., Baharuddin, N. A., Somalu, M. R. and Muchtar, A. (2020). Review of composite cathodes for intermediate-temperature solid oxide fuel cell applications. *Ceramics International,* 46(15): 23314-23325.
5. Tahir, N. N. M., Baharuddin, N. A., Samat, A. A., Osman, N. and Somalu, M. R. (2022). A review on cathode materials for conventional and proton-conducting solid oxide fuel cells. *Journal of Alloys and Compounds,* 894: 162458.
6. Kim, M., Kim, D. H., Han, G. D., Choi, H. J., Choi, H. R. and Shim, J. H. (2020). Lanthanum strontium cobaltite-infiltrated lanthanum strontium cobalt ferrite cathodes fabricated by inkjet printing for high-performance solid oxide fuel cells. *Journal of Alloys and Compounds,* 843: 155806.
7. Rainwater, B. H., Liu, M. and Liu, M. (2012). A more efficient anode microstructure for SOFCs based on proton conductors. *International Journal of Hydrogen Energy,* 37(23): 18342-18348.
8. Dwivedi, S. (2020). Solid oxide fuel cell: Materials for anode, cathode and electrolyte. *International Journal of Hydrogen Energy,* 45(44): 23988-24013.
9. Rosli, A. Z., Somalu, M. R., Osman, N. and Hamid, N. A. (2021). Physical characterization of LSCF-NiO as cathode material for intermediate temperature solid oxide fuel cell (IT-SOFCs). *Materials Today: Proceedings,* 46:1895-1900.
10. Samat, A. A., Somalu, M. R., Muchtar, A. and Osman, N. (2019, June). Electrochemical performance of La0. 6Sr0. 4CoO3-δ cathode in air and wet air for BaCe0.54Zr0.36Y0.1O3-based proton-conducting solid oxide fuel cell. *In IOP Conference Series: Earth and Environmental Science*, 268(1): 012136.
11. Lv, H., Jin, Z., Peng, R., Liu, W. and Gong, Z. (2019). BaCoxFe0. 7-xZr0. 3O3-δ (0.2≤ x≤ 0.5) as cathode materials for proton-based SOFCs. *Ceramics International*, 45(18): 23948-23953.
12. Huan, D., Shi, N., Xie, Y., Li, X., Wang, W., Xue, S., ... and Lu, Y. (2020). Cathode materials for proton-conducting solid oxide fuel cells. *Intermediate Temperature Solid Oxide Fuel Cells*: pp. 263-314.
13. Le, S., Zhu, S., Zhu, X. and Sun, K. (2013). Densification of Sm0. 2Ce0.8O1.9 with the addition of lithium oxide as sintering aid. *Journal of Power Sources,* 222: 367-372.
14. Yuan, L. X., Wang, Z. H., Zhang, W. X., Hu, X. L., Chen, J. T., Huang, Y. H. and Goodenough, J. B. (2011). Development and challenges of $LiFePO_4$ cathode material for lithium-ion batteries. *Energy & Environmental Science,* 4(2): 269-284.
15. Hofmann, T., Westhoff, D., Feinauer, J., Andrä, H., Zausch, J., Schmidt, V. and Mueller, R. (2020). Electro-chemo-mechanical simulation for lithium ion batteries across the scales. *International Journal of Solids and Structures,* 184: 24-39.
16. Janowitz, K., Kah, M. and Wendt, H. (1999). Molten carbonate fuel cell research: Part I. Comparing cathodic oxygen reduction in lithium/potassium and lithium/sodium carbonate melts. *Electrochimica Acta,* 45(7): 1025-1037.
17. Accardo, G., Kim, G. S., Ham, H. C. and Yoon, S. P. (2019). Optimized lithium-doped ceramic electrolytes and their use in fabrication of an electrolyte-supported solid oxide fuel cell. *International Journal of Hydrogen Energy,* 44(23): 12138-12150.
18. Preethi, S., Abhiroop, M. and Babu, K. S. (2019). Low temperature densification by lithium co-doping and its effect on ionic conductivity of samarium doped ceria electrolyte. *Ceramics International,* 45(5): 5819-5828.

19. Kanthachan, J., Khamman, O., Intatha, U. and Eitssayeam, S. (2021). Effect of reducing calcination processing on structural and electrochemical properties of LiNi0.5Mn0.3Co0.2O2 cathode materials for lithium battery. *Materials Today: Proceedings,* 47: 3600-3603.
20. Hu, X., Qiang, W. and Huang, B. (2017). Surface layer design of cathode materials based on mechanical stability towards long cycle life for lithium secondary batteries. *Energy Storage Materials,* 8: 141-146.
21. Peng, Y., Tan, R., Ma, J., Li, Q., Wang, T. and Duan, X. (2019). Electrospun $Li_3V_2(PO_4)_3$ nanocubes/carbon nanofibers as free-standing cathodes for high-performance lithium-ion batteries. *Journal of Materials Chemistry A*, 7(24): 14681-14688.
22. Yan, R., Oschatz, M. and Wu, F. (2020). Towards stable lithium-sulfur battery cathodes by combining physical and chemical confinement of polysulfides in core-shell structured nitrogen-doped carbons. *Carbon,* 161, 162-168.
23. Zhang, L., Lan, R., Kraft, A., Wang, M. and Tao, S. (2010). Cost-effective solid oxide fuel cell prepared by single step co-press-firing process with lithiated NiO cathode. *Electrochemistry Communications,* 12(11): 1589-1592.
24. Hussain, S. and Yangping, L. (2020). Review of solid oxide fuel cell materials: Cathode, anode, and electrolyte. *Energy Transitions*, 4(2): 113-126.
25. Hou, J., Miao, L., Hui, J., Bi, L., Liu, W. and Irvine, J. T. (2018). A novel in situ diffusion strategy to fabricate high performance cathodes for low temperature proton-conducting solid oxide fuel cells. *Journal of Materials Chemistry A,* 6(22): 10411-10420.
26. Yuan, K., Yu, Y., Wu, Y., Ji, X., Xu, Z. and Shen, J. (2018). Plasma sprayed coatings for low-temperature SOFC and high temperature effects on Lix (Ni, Co) yO_2 catalyst layers. *International Journal of Hydrogen Energy,* 43(28): 12782-12788.
27. Wan Yusoff, W. N. A., Somalu, M. R., Baharuddin, N. A., Muchtar, A. and Wei, L. J. (2020). Enhanced performance of lithiated cathode materials of $LiCo0.6X0.4O_2$ (X= Mn, Sr, Zn) for proton-conducting solid oxide fuel cell applications. *International Journal of Energy Research,* 44(14): 11783-11793.
28. Yusoff, W. N. A. W., Norman, N. W., Samat, A. A., Somalu, M. R., Muchtar, A. and Baharuddin, N. A. (2019). Performance of $LiCo0.6Zn0.4O_2$ as a potential cathode material candidate for intermediate solid oxide fuel cell application. *In IOP Conference Series: Earth and Environmental Science*, 268(1): 012139.
29. Zhang, Y., Yang, G., Chen, G., Ran, R., Zhou, W. and Shao, Z. (2016). Evaluation of the CO_2 poisoning effect on a highly active cathode SrSc0.175Nb0.025Co0.8O3-δ in the oxygen reduction reaction. *ACS Applied Materials & Interfaces,* 8(5): 3003-3011.
30. Jamil, S. M., Othman, M. H. D., Rahman, M. A., Jaafar, J., Mohamed, M. A., Yusop, M. Z. M., ... and Tanemura, M. (2017). Dual-layer hollow fiber MT-SOFC using lithium doped CGO electrolyte fabricated via phase-inversion technique. *Solid State Ionics,* 304: 113-125.
31. Ratso, S., Zitolo, A., Käärik, M., Merisalu, M., Kikas, A., Kisand, V., ... and Tammeveski, K. (2021). Non-precious metal cathodes for anion exchange membrane fuel cells from ball-milled iron and nitrogen doped carbide-derived carbons. *Renewable Energy,* 167: 800-810.
32. Olowojoba, G., Sathyanarayana, S., Caglar, B., Kiss-Pataki, B., Mikonsaari, I., Hübner, C. and Elsner, P. (2013). Influence of process parameters on the morphology, rheological and dielectric properties of three-roll-milled multiwalled carbon nanotube/epoxy suspensions. *Polymer,* 54(1): 188-198.
33. Böttcher, A. C., Thon, C., Fragnière, G., Chagas, A., Schilde, C. and Kwade, A. (2021). Rigidly-mounted roll mill as breakage tester for characterizing fine particle breakage. *Powder Technology,* 383: 554-563.

34. Abdul, S. A., Yusoff, W. N. A. W., Baharuddin, N. A., Somalu, M. R., Muchtar, A. and Osman, N. (2018). Electrochemical performance of sol-gel derived La0.6S0.4CoO3-δ cathode material for proton-conducting fuel cell: A comparison between simple and advanced cell fabrication techniques. P*rocessing and Application of Ceramics,* 12(3): 277-286.
35. Somalu, M. R., Muchtar, A., Daud, W. R. W. and Brandon, N. P. (2017). Screen-printing inks for the fabrication of solid oxide fuel cell films: a review. *Renewable and Sustainable Energy Reviews,* 75: 426-439.
36. Sun, G., Yu, F. D., Zhao, C., Yu, R., Farnum, S., Shao, G., ... and Wang, Z. B. (2021). Decoupling the voltage hysteresis of Li-rich cathodes: electrochemical monitoring, modulation anionic redox chemistry and theoretical verifying. *Advanced Functional Materials,* 31(1): 2002643.